

# Fiber Bragg grating multi-chemical sensor

Patrick Boland<sup>\*a</sup>, Gopakumar Sethuraman<sup>a</sup>, Alexis Mendez<sup>b</sup>, Tom Graver<sup>c</sup>, Dmitry Pestov<sup>d</sup>, and Gregory Tait<sup>a</sup>

<sup>a</sup>Electrical Engineering Department, Virginia Commonwealth University, Richmond, VA 23284

<sup>b</sup>MCH Engineering, LLC, 1728 Clinton Avenue, Alameda, California 94501

<sup>c</sup>Micron Optics, Inc., 1852 Century Place, Atlanta, Georgia 30345

<sup>d</sup>Sentor Technologies Inc., 11551 Nuckols Road, Suite Q, Glen Allen, Virginia 23060

## ABSTRACT

Fiber optic-based chemical sensors are created by coating fiber Bragg gratings (FBG) with the glassy polymer cellulose acetate (CA). CA is a polymeric matrix capable of localizing or concentrating chemical constituents within its structure. Some typical properties of CA include good rigidity (high modulus) and high transparency. With CA acting as a sensor element, immersion of the gratings in various chemical solutions causes the polymer to expand and mechanically strain the glass fiber. This elongation of the fiber sections containing the grating causes a corresponding change in the periodicity of the grating that subsequently results in a change in the Bragg-reflected wavelengths. A high-resolution tunable fiber ring laser interrogator is used to obtain room-temperature reflectance spectrograms from two fiber gratings at two different wavelengths – 1540nm and 1550nm. The graphical representation from this device enables the display of spectral shape, and not merely shifts in FBG central wavelength, thereby allowing for more comprehensive analysis of how different physical conditions cause the reflectance profile to move and alter overall form. Shifts on the order of 1 to 80 pm in the FBG central wavelength and changes in spectral shape are observed in both sensors upon immersion in a diverse selection of chemical analytes.

**Keywords:** Bragg gratings, fiber optic, polymer, chemical sensor, reflectance

## 1. INTRODUCTION

This study builds on our previous work and focuses on the use of fiber Bragg grating (FBG) sensors to detect various chemicals commonly found in microelectronics cleanrooms and industrial settings and selected Toxic Industrial Chemicals (TICs) – all in the liquid phase.<sup>1</sup> The effectiveness of a common polymer is being investigated for its suitability as a transducer element when applied directly to the cladding of a fiber containing a single Bragg grating. Specific characteristics of interest when using this type of sensor include reagentless chemical detection, reproducibility of results, and the relation of chemical properties to spectral changes. This work addresses polymer application to the fiber, spectral responses of the test FBGs, and analyses of test results obtained.

FBGs are used as sensors to measure many types of physical phenomena including strain, temperature, vibration, humidity, and pressure in a variety of diverse applications. A few of these include bridge and mine stress measurements, marine vehicle pressures, and aircraft stress assessment.<sup>2-5</sup> Use of FBGs as chemical sensors is less prevalent. In our applications, a polymer coating is applied to the fiber so that interaction with target chemicals produces a swelling of the polymer and subsequent straining of the fiber and FBG contained within. This elongation of the fiber causes an increase in Bragg period ( $\Lambda_B$ ) and a resultant shift in Bragg reflectance wavelength ( $\lambda_B$ ). This project examines sensor response to several analytes including isopropanol, gasoline, hydrochloric acid, ammonium hydroxide, ethanol, hydrogen peroxide, sodium solution, oxalic acid, ethylene glycol, sodium hypochlorite, potassium hydroxide, methylene chloride, methyl sulfoxide, acetonitrile, and dimethylformamide and reports on spectral changes in relation to chemical properties.

\*bolandpm@vcu.edu

## 2. CHEMICAL SENSOR

The chemical sensor in this study was developed using a polymer applied to the fiber cladding to form a transducer that, upon exposure to various chemicals, expands in size and exerts strain on the underlying fiber. Cellulose acetate (CA), a glassy polymer with a high Young's modulus, strongly adheres to the cladding ensuring physical deformation of the polymer is transferred to the glass fiber. This strain is simultaneously applied to the FBG contained in the fiber core and the axial elongation increases the Bragg period ( $\Lambda_B$ ) that is related to the Bragg wavelength ( $\lambda_B$ ) according to the equation:

$$\lambda_B = 2 n_{\text{eff}} \Lambda_B \quad (1)$$

This increase in Bragg period results in an increase in the Bragg (reflectance) wavelength and a shift to longer wavelengths on a spectral display.<sup>6-9</sup> A benefit of this type of sensor is that no alteration of the fiber structure, such as stripping the cladding, or modification of its inherent effective index of refraction ( $n_{\text{eff}}$ ) is required. This ensures that mechanical strength is not degraded and structural integrity is maintained. This is important considering the harsh environments in which sensors of this type would be employed (e.g. high vibration, temperature, strain, etc.).

Cellulose acetate is produced by treating cellulose with acetic anhydride and pyridine.<sup>10</sup> The chemical reaction is shown in Fig. 1.

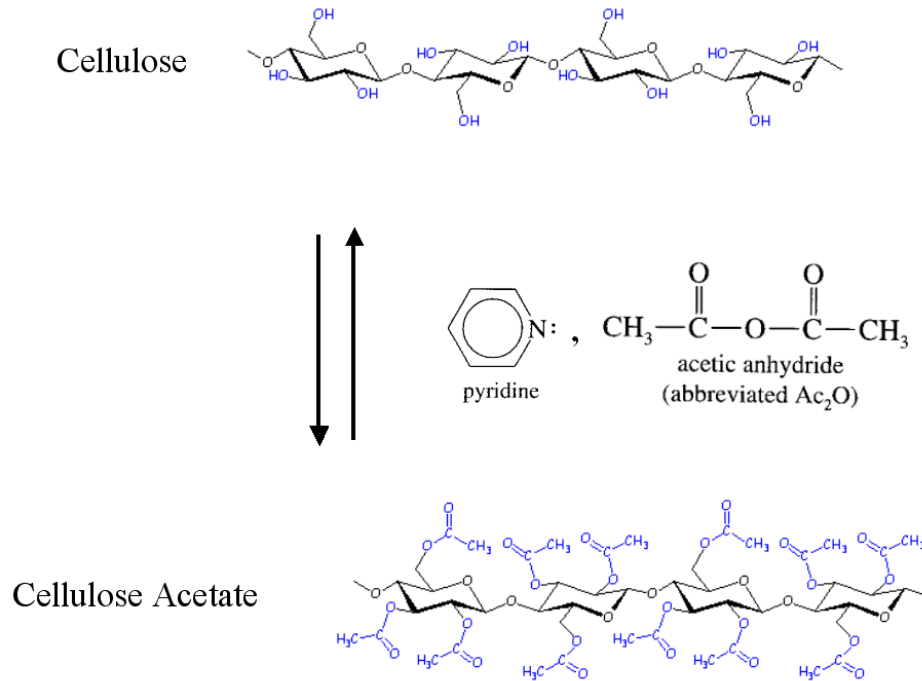


Fig. 1. Synthesis of cellulose acetate.<sup>11-12</sup>

The effect of combining these reactants is to eliminate the ability of cellulose to hydrogen-bond – a property that allows it to remain stiff and very strong by bonding to other cellulose molecules. Hydrogen bonding takes place at the side-chains on the hydroxyl groups (-OH). Pyridine and acetic anhydride cause a reaction whereby the hydroxyl groups are blocked from any further hydrogen bonding. The resulting polymer, cellulose acetate, has chains that are more spread out, much less rigid, and able to fold in upon itself and tangle with other chains to create a matrix.<sup>13</sup> It is this matrix that can now be cast into a film that concentrates various chemicals subject to several parameters involving *selectivity* of the polymer.

Polymers demonstrate selectivity to various analytes based on physicochemical properties. These properties are often described using 3-D models, of which the most popular in use today was developed by Hansen.<sup>14</sup> The Hansen parameters are 1) a dispersion force component  $\delta_d^2$ , 2) a polar component  $\delta_p^2$ , and 3) a hydrogen-bonding component  $\delta_h^2$ .

Hansen's 3-D model is shown in Fig. 2.

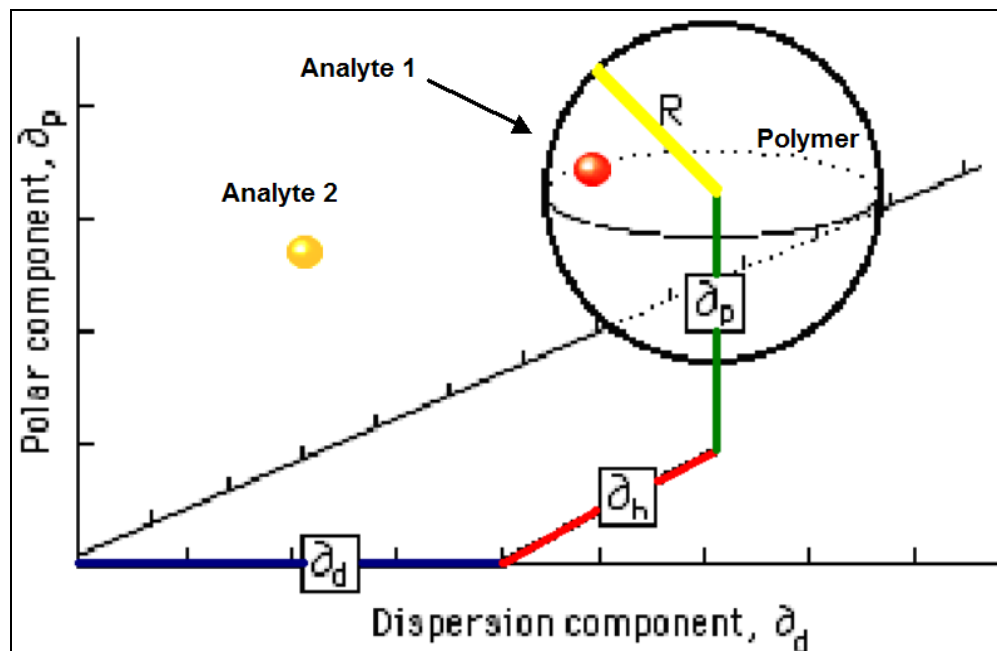


Fig. 2. Hansen's 3-D model for plotting polymer solubilities.<sup>14-16</sup>

The volume of the sphere in Hansen's model represents the solubility of a polymer where Hansen's parameters determine the center of the sphere and  $R$  is the radius of interaction.  $R$ -values and associated Hansen parameters are listed in solubility tables and are available for many polymers. Hansen parameters are also available for analytes and a correlation between the radii of the polymer and analyte exists that affects absorption and swelling. For example, to determine if a particular organic analyte will be absorbed, the distance of the solvent to the center of Hansen's sphere needs to be calculated using the following equation:

$$D_{(S-P)} = [4(\delta_{dS} - \delta_{dP})^2 + (\delta_{pS} - \delta_{pP})^2 + (\delta_{hS} - \delta_{hP})^2]^{1/2} \quad (2)$$

where

$D_{(S-P)}$  = Distance between solvent and center of polymer solubility sphere,

$\delta_{xS}$  = Hansen component parameter for solvent,

and

$\delta_{xP}$  = Hansen component parameter for polymer

In equation (2), the factor "4" is based on empirical data. If  $D_{(S-P)} \leq R$ , the analyte will be absorbed and the polymer will swell. In Fig. 2, Analyte 1 will cause a high degree of swelling, but the effect of Analyte 2 will be less. For inorganic analytes such as acids and bases, a different approach is required. Depending on the selection of target analyte, polymers having the appropriate functional groups in the side chains would be needed to obtain the desired selectivity. Examples of some target analytes and their suitable polymers are listed in Table 1.

Table 1. Target analytes and suitable polymers.

<u>ANALYTE</u>	<u>POLYMER</u>
Ammonia	Copolymer of acrylic monomers – methacrylic acid
Nitric acid, sulfuric acid, HCl, HBr	Acrylic copolymers with N,N-dimethylaminoethyl methacrylate
Gasoline (as an emulsion or pure liquid)	Methacrylate-ethylene copolymer
Formaldehyde	Polyethylene terephthalate (PET)

In developing this type of sensor, polymers demonstrating a high degree of swelling under test conditions are desirable. The polymer should also be rigid (high Young's modulus) in order to produce enough stress on the glass fiber so that a sufficient level of strain is imparted to the FBG. In addition, polymers with controlled cross-linking are a good choice as they can be used in harsh conditions and have a long lifetime.<sup>13-14</sup>

In this work, CA is applied to two glass fibers – each containing a single FBG. Fiber 1 and fiber 2 have a measured Bragg wavelength ( $\lambda_B$ ) of 1540.41nm and 1550.36nm, respectively. Measured reflectivities are 99.7% and 90.5%. The polymer was applied directly over the inscribed FBGs at room temperature and then allowed to dry for about 20 minutes. A CA-coated fiber Bragg grating is depicted in Fig. 3.

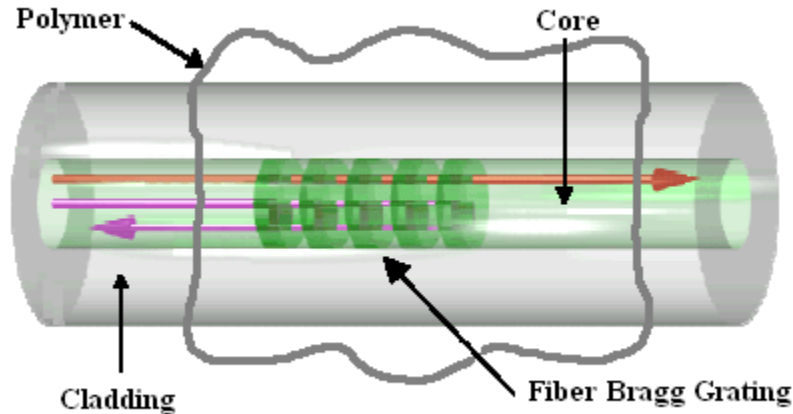


Fig. 3. Polymer-coating on fiber containing a single Bragg grating.

### 3. OPTICAL INTERROGATOR

A state-of-the-art unit containing a swept fiber laser source and large-dynamic-range photodetectors (Micron Optics model si720-500) is used to interrogate and demodulate reflected optical signals from both FBGs simultaneously. This instrument allows real-time, full-spectrum data acquisition and easy data transfer to a PC via an Ethernet remote utility. With the sweep rate set to 5Hz, a 50nm spectrum could be observed thereby displaying the entire reflectance profile.<sup>17</sup>

To accomplish the data collection, the optical fibers are attached to mounts with the FBG-containing portion of the glass suspended above a petri dish. The petri dish is used to contain the liquid analytes under test. The distant ends of the fibers are terminated with small-radius, 180-degree bends and immersion in index-matching fluid. The opposite ends of each fiber are connected to a 2x2 fiber coupler and then subsequently to the “Laser Out” and “Detector” interfaces on the swept laser interrogator unit. After initial instrument calibration, baseline measurements of each fiber are made in air. Each of the two reflection spectrograms were compared with factory-provided data sheets for the FBGs and found to be in very close agreement.

For each of the chemicals tested, the petri dish is filled with a chemical solution, the FBG immersed in the dish, the power vs. wavelength measurement (reflection spectrogram) obtained, and the data saved in Microsoft Excel spreadsheet format. Between the test of each analyte, deionized water is used to clean both the fiber and petri dish.

The experimental setup is shown in Figs. 4 and 5.

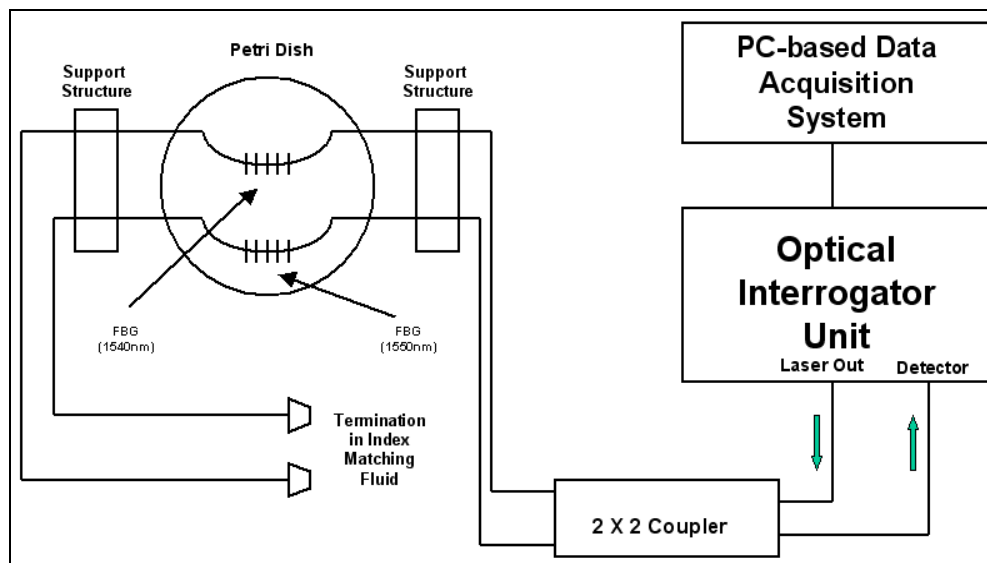


Fig. 4. Schematic – optical interrogation with swept laser interrogator and PC-based data acquisition software.

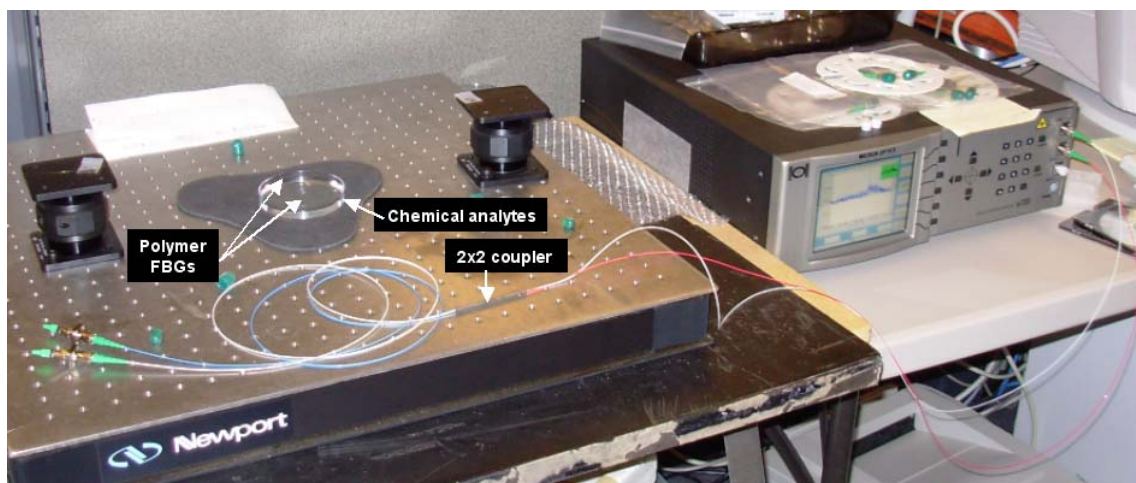


Fig. 5. Swept laser FBG interrogator (Micron Optics model si720-500) and test bench.

## 4. RESULTS

After cleaning the cladding with tetrahydrofuran (THF), the thick CA is applied directly to the glass without additional chemical modification (e.g. use of silane to promote adhesion) of the fiber surface. The CA does not adhere to the fiber in a uniform fashion, but rather presents a striated and non-uniform appearance upon inspection under the microscope as can be seen in Fig. 6. In the future, a selection of chemical agents will be tried in order to achieve better adhesion and a smoother surface.

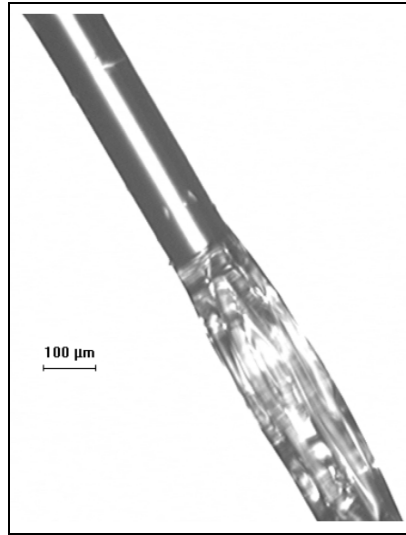


Fig. 6. CA-coated FBG with striated surface.

Both sensors were tested using the analytes listed in Table 2.

Table 2. Analytes tested.

FIBER 1 (1540nm)	FIBER 2 (1550nm)	
Water (deionized)	Water (deionized)	Ethanol (50%)
Hydrogen peroxide (3%)	Hydrogen peroxide (3%)	Dimethylformamide
Sodium chloride solution (0.9%)	Sodium chloride solution (0.9%)	Gasoline (87 Octane)
Ammonium Hydroxide (<21%)	Ammonium Hydroxide (<21%)	Acetonitrile
Isopropanol (70%)	Isopropanol (70%)	Ethylene Glycol
Isopropanol w/Methyl Salicylate (70%)	Isopropanol w/Methyl Salicylate (70%)	Methyl Sulfoxide
Ethanol (100%)	Ethanol (100%)	Methylene Chloride
Potassium Hydroxide (20%)	Potassium Hydroxide (20%)	
Oxalic Acid (10%)	Oxalic Acid (10%)	
Hydrochloric acid (HCl) (1M)	Sodium Hypochlorite (5.25%)	

The following series of graphs show results obtained for both sensors. Fiber 1 has a measured center wavelength of 1540.41 nm and reflectivity of 99.7% while the values for Fiber 2 are 1550.36 nm and 90.5%. Figures 7 (a) and (b) show the spectrograms for both sensors in air after application of CA to the fiber.

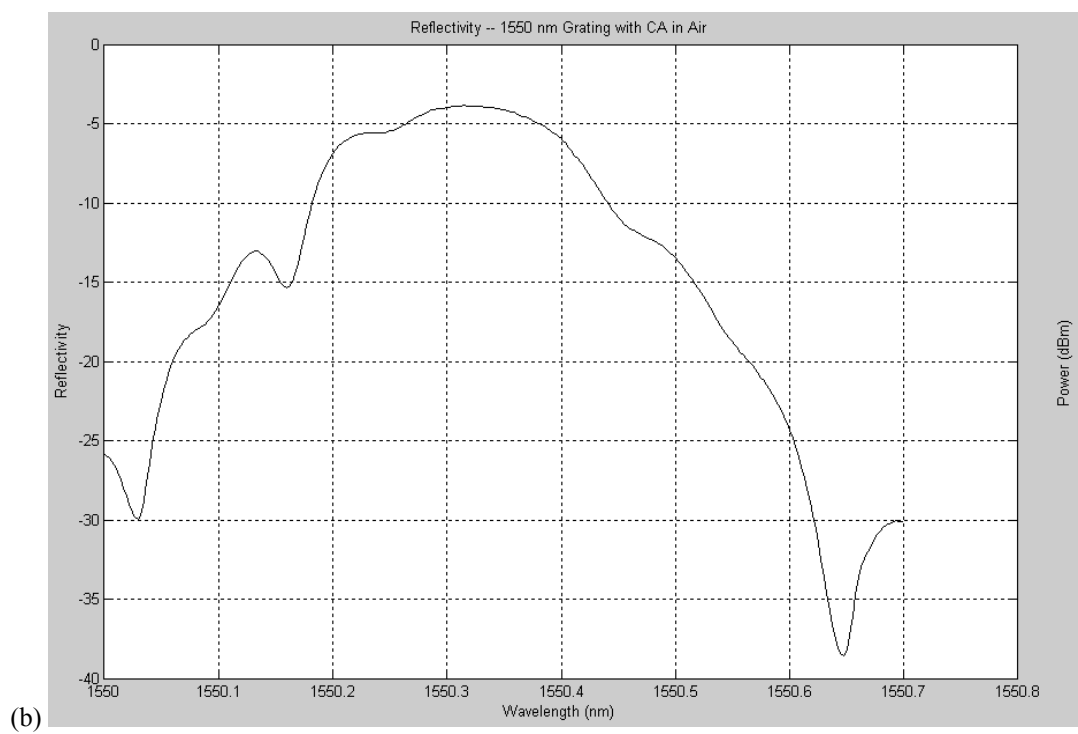
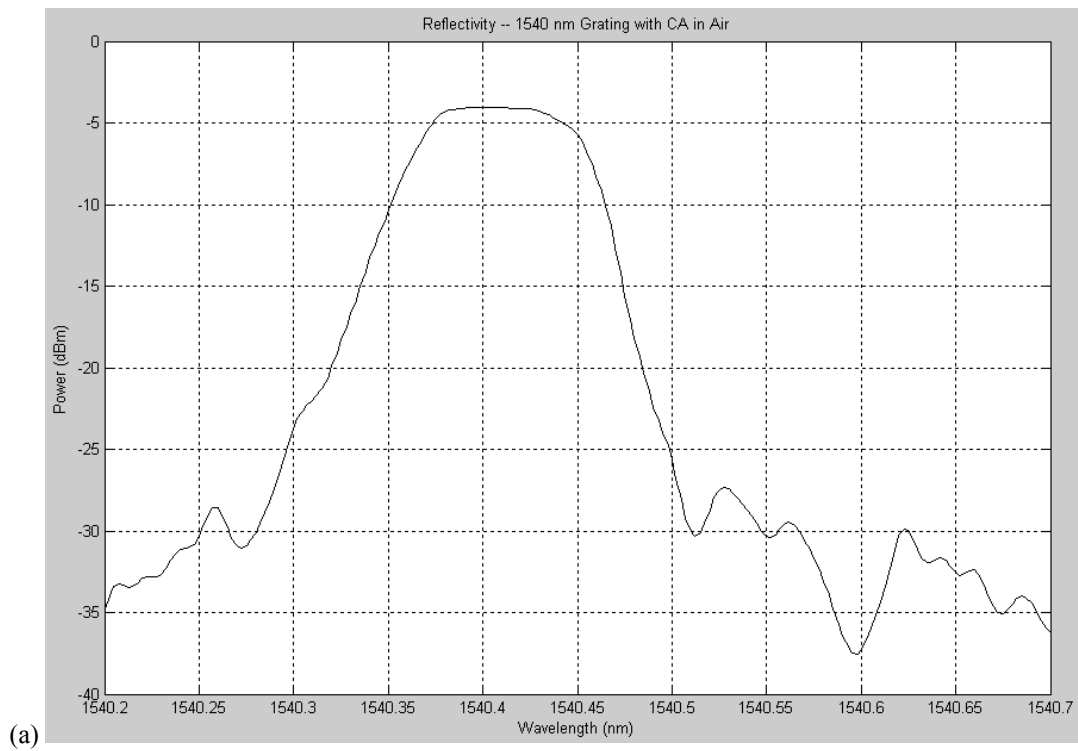


Fig. 7. Measured reflectivities in air for coated CA gratings at a) 1540 nm, and b) 1550 nm.

In Fig. 8, spectral results are shown for analytes tested using the 1540 nm sensor.

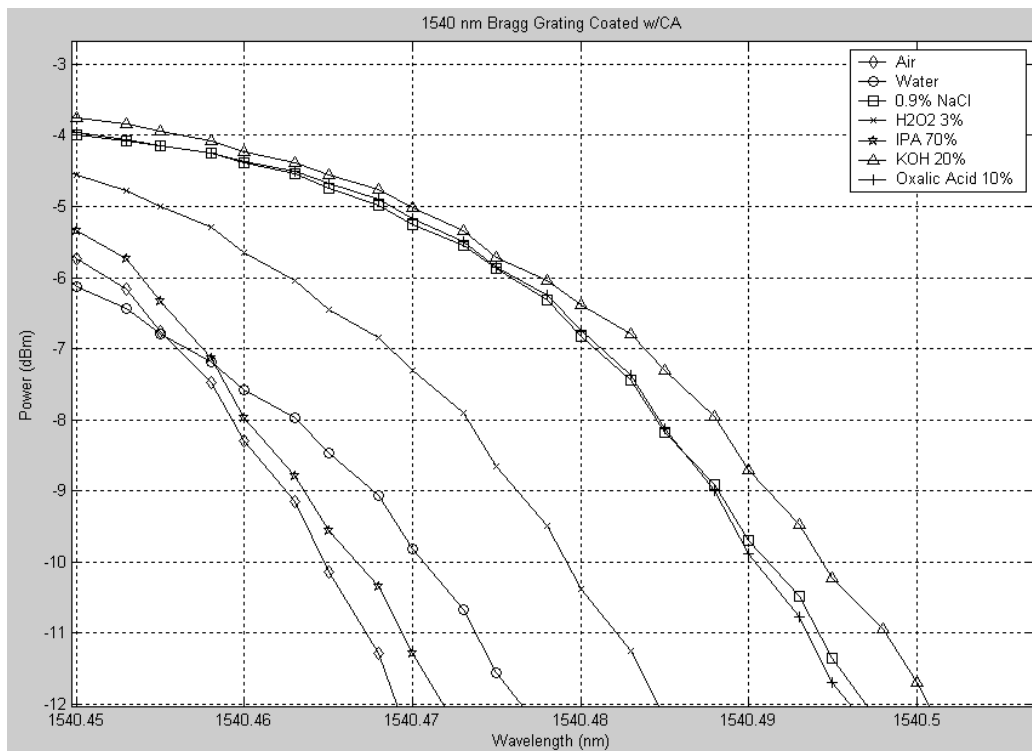


Fig. 8. Right-edge transitions for 1540nm polymer-coated FBG.

The response of the sensor in Fiber 2 is shown in Figs. 9 through 12. All figures show right-edge transitions.

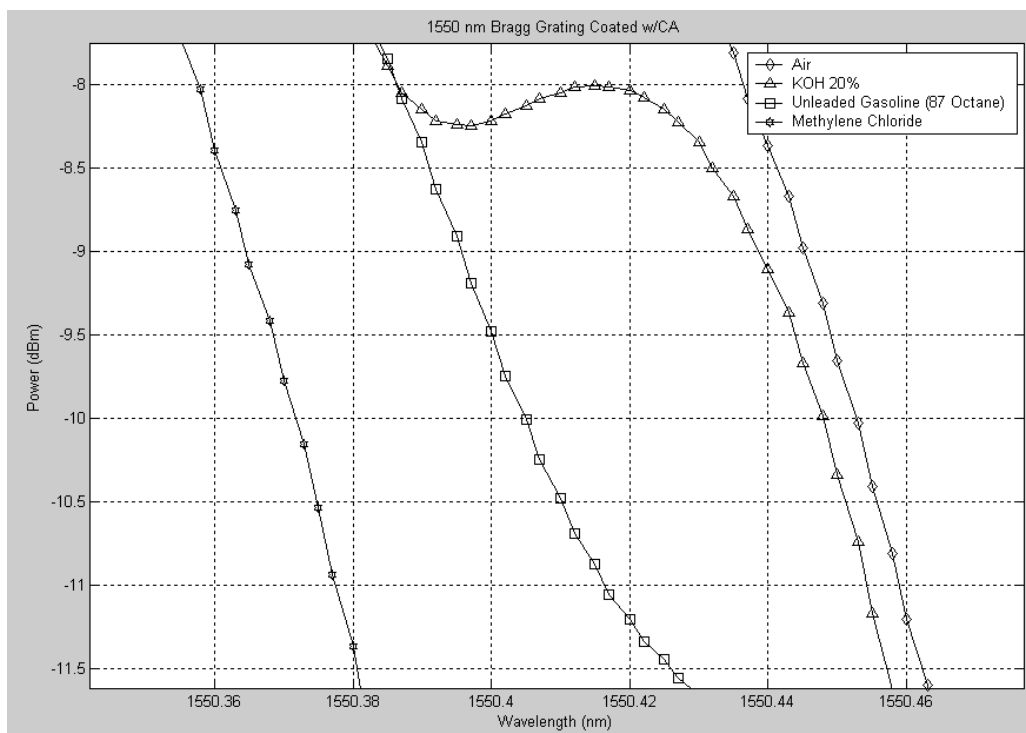


Fig. 9. Right-edge transitions for 1550nm polymer-coated FBG (Screen 1 of 4).



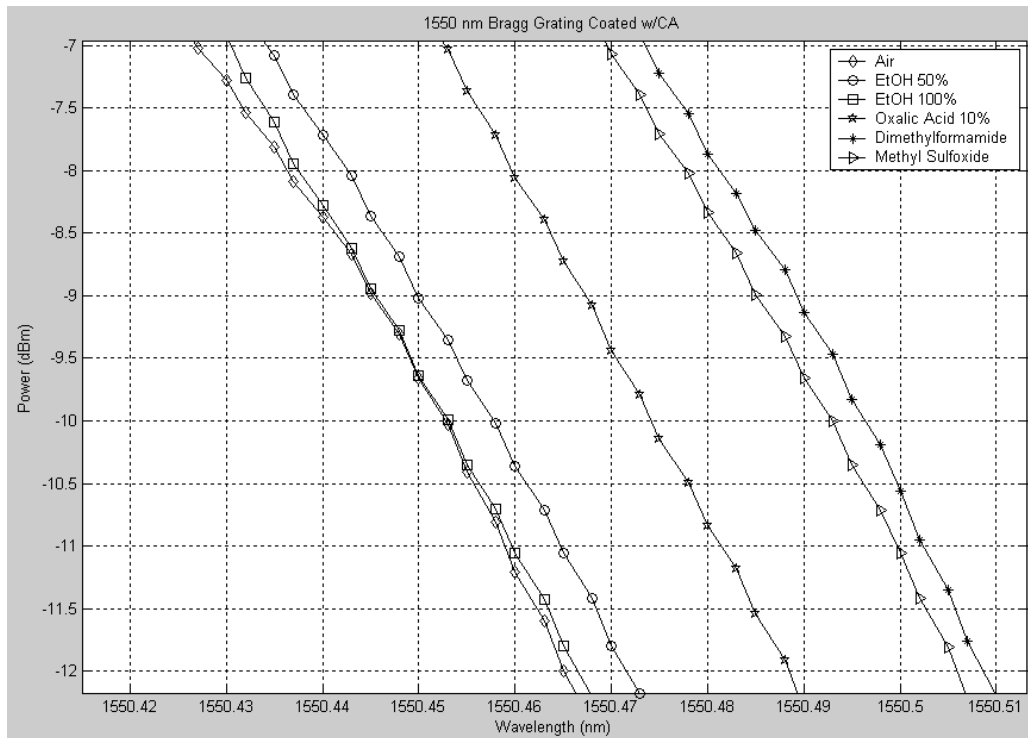


Fig. 10. Right-edge transitions for 1550nm polymer-coated FBG (Screen 2 of 4).

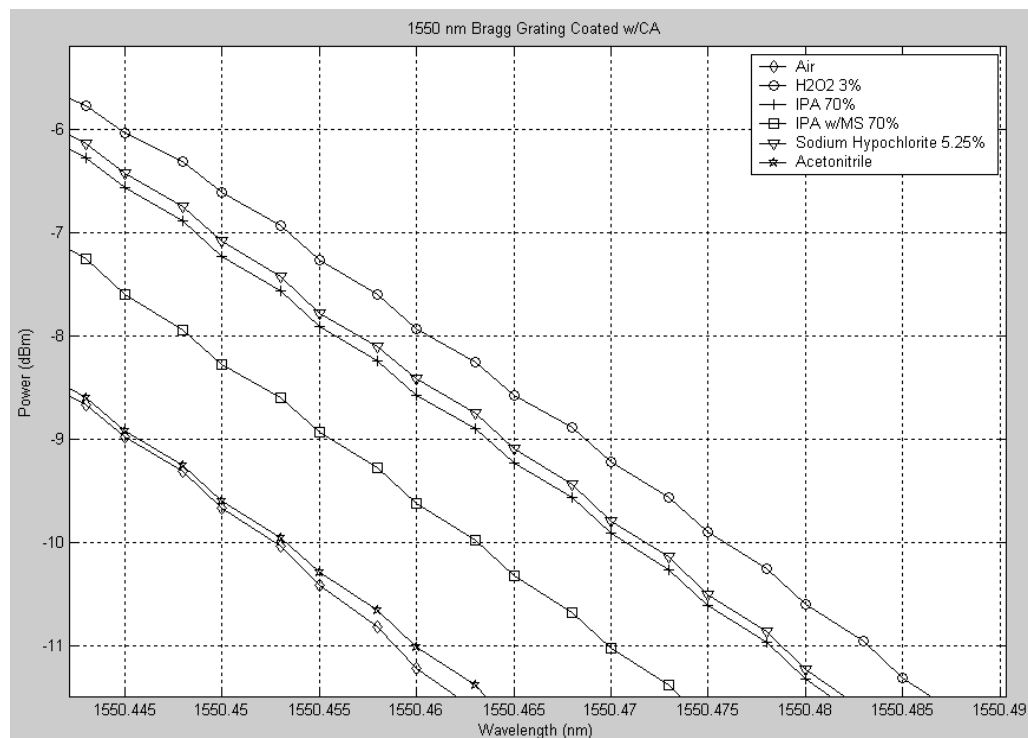


Fig. 11. Right-edge transitions for 1550nm polymer-coated FBG (Screen 3 of 4).

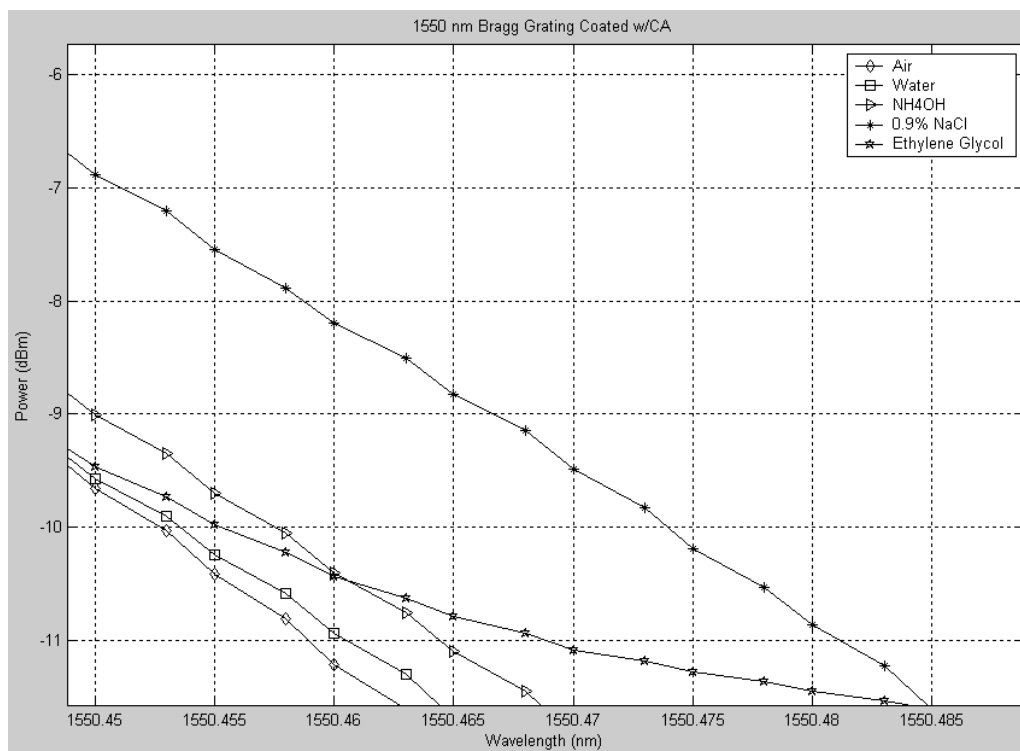


Fig. 12. Right-edge transitions for 1550nm polymer-coated FBG (Screen 4 of 4).

Figures 9 through 12 show wavelength shifts ranging from approximately 1 to 80 pm. The sensitivity is based on the minimum resolution obtainable with this particular experimental setup and is a function of the polymer swelling characteristic, the transfer of strain to the underlying grating, tunability of the laser, and averaging and interpolating algorithms of the signal processing. As a conservative estimate, shifts of 1 pm are easily resolvable. Given the ranges observed during the experimental procedure, it's clear that multi-chemical detection is possible with an excellent degree of accuracy. After removing the sensor from each analyte, cleaning with deionized water, and allowing the polymer to air dry, the spectrograms are observed to return to the nominal "in-air" baseline. This demonstrates the reversibility and reuseability of the sensor. Work is underway to determine the effects of the analyte concentration properties of the polymer on sensitivity.

## 5. CONCLUSION

This work explores polymer-coated FBG sensors and demonstrates their reagentless, reversible, and reusable operation. Bragg grating sensors are capable of sensing a multiplicity of chemicals with a single sensor and can be used in near real time and remotely at great distances due to the low-loss fiber optic. In addition, they have other desirable characteristics including being lightweight, small, inexpensive and immune to vibration, EMI and explosive atmospheres. Graphical representations of the data from this study show not only shifts in FBG central wavelength, but also changes in spectral shape. These representations allow for more comprehensive analyses of how different chemicals cause the reflectance profiles to shift and alter overall form. Further analysis will be required to understand the mechanisms causing these changes and how they may be exploited to improve FBG sensor technology.

## REFERENCES

1. G.B.Tait, G.C.Tepper, D.Pestov, and P.M.Boland, "Fiber Bragg grating multi-functional chemical sensor," Proceedings, 2005 SPIE International Symposium Optics East (Boston, MA), October 2005.
2. Y.J.Rao, "Recent progress in applications of in-fibre Bragg grating sensors," *Optics Lasers Eng.*, **31**, 297-324 (1999).
3. T.L.Yeo, T.Sun, K.T.V.Grattan, D.Parry, R.Lade, and B.D.Powell, "Characterisation of a polymer-coated fibre Bragg grating sensor for relative humidity sensing," *Sensors and Actuators B*, **110**, 148-155 (2005).
4. A.D.Kersey, M.A.Davis, H.J.Patrick, M.LeBlanc, K.P.Koo, C.G.Askins, M.A.Putnam, and E.J.Friebele, "Fiber Grating Sensors," *IEEE J. Lightwave Tech.*, **15** (8), 1442-1463 (1997).
5. I.C.Song, S.K.Lee, S.H.Jeong, and B.H.Lee, "Absolute Strain Measurements Made with Fiber Bragg Grating Sensors," *Applied Optics*, **43** (6), 1337-1341 (2004).
6. A.Othonos and K. Kalli, *Fiber Bragg Gratings Fundamentals and Applications in Telecommunications and Sensing*. Boston: Artech House, 1999.
7. R.Kashyap, *Fiber Bragg Gratings*. San Diego: Academic Press, 1999.
8. T.Erdogan, "Fiber Grating Spectra," *IEEE J. Lightwave Tech.*, **15** (8), 1277-1294 (1997).
9. K.O.Hill and G.Meltz, "Fiber Bragg Grating Technology Fundamentals and Overview," *IEEE J. Lightwave Tech.*, **15** (8), 1263-1276 (1997).
10. L.G. Wade Jr., *Organic Chemistry*, 4<sup>th</sup> ed., Prentice Hall, 1999, p. 1100.
11. Ibid., 983. (acetic anhydride).
12. Ibid., 856. (pyridine).
13. *Chemical Modification of Cellulose*, <http://pslc.ws/fire/cellulos/chemmod.htm>.
14. J.Burke, *SolubilityParameters: Theory and Application*, <http://palimpsest.stanford.edu/byauth/burke/solpar/solpar6.html>.
15. D.Pestov, (private communication).
16. A. Barton, *Handbook of Solubility Parameters and Other Cohesion Parameters*. Boca Raton, FL: CRC Press Inc., 1983.
17. Micron Optics, Inc., "si720 Swept Laser Interrogator Instruction Manual," November, 2003.